# Supporting Information

## Table of Contents:

**Experimental Procedures**

**General Remarks.** All solvents and reagents were purchased from commercial sources and used as received unless otherwise stated. $^{1}$H CEST spectra, relaxation studies, and $^{13}$C NMR were recorded on a Varian VNMRS direct drive Varian console spectrometer operating at 400 and 100 MHz respectively. The $^{17}$O spectra were obtained using a Varian 400 MHz Mercury spectrometer. The relaxivity measurements were performed on a Bruker Minispec MQ60 instrument operating at 1 T. Imaging was performed on an Agilent 9.4 T horizontal bore small animal imaging system using a 40 mm volume coil. Cyclic voltammetry was performed on a BAS Epsilon Electrochemical Workstation with glassy carbon as working electrode, Pt wire as counter electrode, $Ag^{+}$/AgCl as reference electrode, and potassium chloride as supporting electrolyte. The voltage sweep rate for each scans were 100 mV.

**Correlation between relaxation rates and the CEST effect**

Samples containing $Eu^{3+}DOTA(gly)_4$ (10 mM) and varying concentrations of GdDOTA as shown in **Table S1** were prepared. 300 µL of each solution were inserted into a vial (2mm diameter, 2 cm length and were placed and arranged in a phantom (1 cm diameter, 3 cm length), which was placed horizontally in the imaging system. The $T_1$w ($T_1$ weighted) images were obtained using a GEMS sequence with: TR = 9.9 ms, TE = 5.0 ms, flip angle of 20°, data matrix of 256 x 256, a FOV of 30 x 30 mm$^2$, 4 averages and a total acquisition time of 10 seconds. The $T_1$map was acquired using a FLAIR sequence with a TR of 4 s, ESP = 10 ms, ETL = 8 kzero = 4, effective TE = 40 ms and a total acquisition time of 4 minutes 24 seconds. The CEST images were obtained using a FSEMS sequence with the same slice settings as described earlier, and the experimental conditions as follows, TR = 3 s, TE = 7 ms, saturation time of 3 s, saturation power 10 µT and a total acquisition time of 4 minutes 30 seconds. The images were collected by at on resonance at 54 ppm and off resonance at -54 ppm and the final image is obtained as a difference image (off resonance – on resonance).

**Table S1.** Relaxation rates and CEST effect of in samples containing varying concentrations of $Gd^{3+}DOTA$ and $Eu^{3+}DOTA(gly)_4$

| **Vial** | **[GdDOTA]** | **[$Eu^{3+}DOTA(gly)_4$]** | **$R_1$** | **CEST effect** |
|---|---|---|---|---|
| | mM | mM | $s^{-1}$ | % |
| 1 | 0 | 10 | 0.5 | 27.2 |
| 2 | 0.1 | 10 | 0.8 | 22.5 |
| 3 | 0.2 | 10 | 1.2 | 18.1 |
| 4 | 0.5 | 10 | 2.2 | 11.2 |
| 5 | 1 | 10 | 3.8 | 6.6 |
| 6 | 1.5 | 10 | 5.4 | 4.7 |
| 7 | 2 | 10 | 7.2 | 3.6 |
| 8 | 4 | 10 | 14.2 | 1.7 |
| 9 | 8 | 0 | 28.0 | 0 |
| 10 | $H_2O$ only | | 0 | |

## Synthesis and characterization of $Eu^{2+}$ complexes

### Synthesis

The synthesis of the ligands DOTA(gly)$_4$ and DOTA were reported previously.[1,2] The complexation was performed in a glove box under $N_2$ atmosphere at room temperature. All solvents were degassed prior use. The $Eu^{2+}$ complexes were prepared without the use of electrochemical methods[3] by adding a solution of the ligand (approx. 0.1 M, 25 to 30 % excess, pH 6) to a vial containing $EuCl_2$ (Sigma-Aldrich, anhydrous) and adjusting the pH back to 6 with NaOH (0.5 M).

### Characterization

The $^1$H NMR spectra and relaxation rates for the $H_2O$ and the ligand resonances of $Eu^{2+}$DOTA(gly)$_4$ and $Eu^{2+}$DOTA were measured over time. The samples were prepared in degassed water at pH =7 in a glove box at the same time, put into 3 mm NMR tubes and sealed. The $T_1$ relaxation times were measured at 20°C over a period of 104 days for $Eu^{2+}$DOTA(gly)$_4$ and 44 days for $Eu^{2+}$DOTA. The natural logarithm was taken of the water relaxation rates to determine a first order decay process of $Eu^{2+}$ to $Eu^{3+}$ with a rate constant of 0.0015 ± 0.0001 $h^{-1}$ and an $A_0$ of 191.1 ± 0.1 $s^{-1}$, for $Eu^{2+}$DOTA(gly)$_4$ and 0.0044 ±0.0001 $h^{-1}$ and $A_0$ of 28.3 ±0.9 $s^{-1}$ for $Eu^{2+}$DOTA, which allowed calculation of the half-lives and relaxivity.

**Relaxivity measurements**

**Relaxivity measurements at 9.4 T**

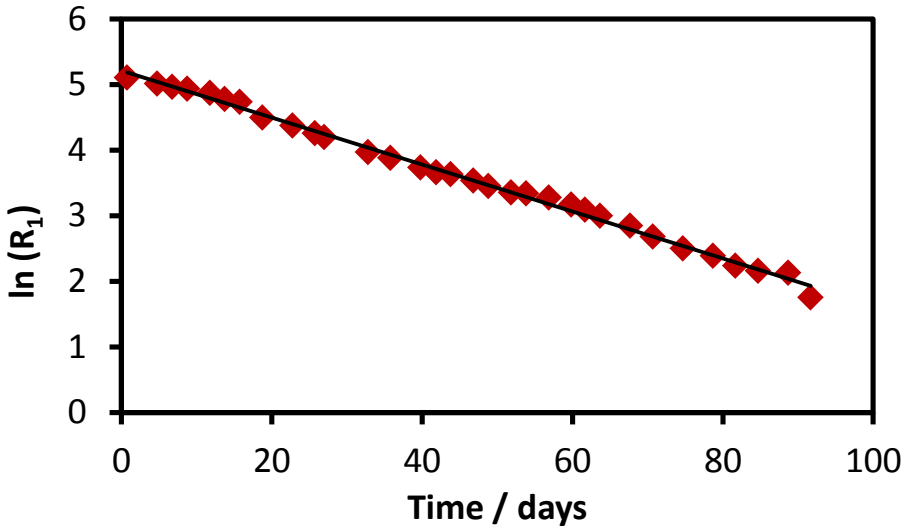


**Figure S1.** The plot of the natural logarithm of the water relaxation rates decay on a 9.4 T NMR of a 60 mM $Eu^{2+}DOTA(gly)_4$ in a closed system stored under inert atmosphere.

**Relaxivity measurements at 1 T**

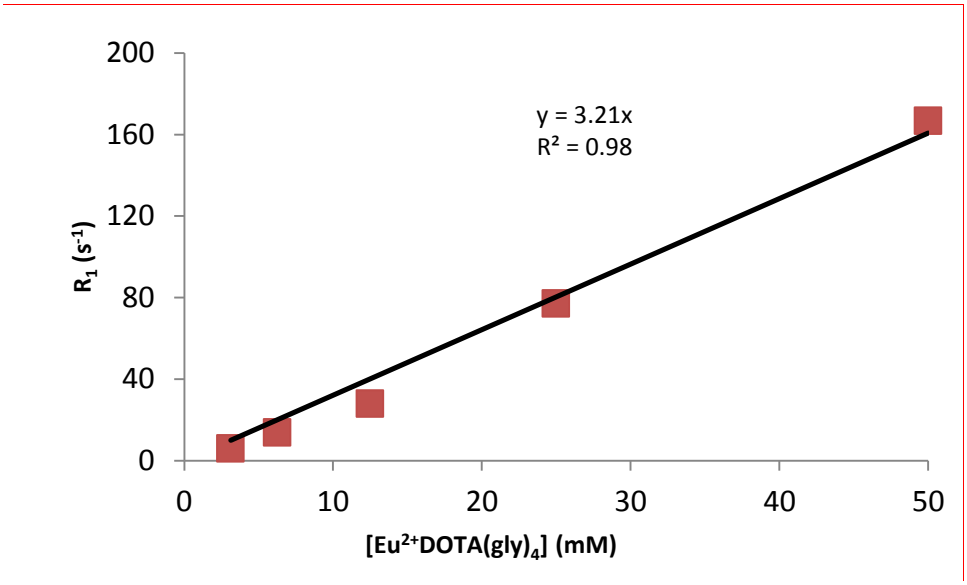


**Figure S2**. The plot of the concentration of $Eu^{2+}DOTA(gly)_4$ complex versus the relaxation rate measured at 1 T in water at pH 7.

**Water exchange rates ($k_{ex}$)**

The $^{17}O$ linewidths of both $Eu^{2+}DOTA(gly)_4$ and $Eu^{2+}DOTA$ were measured on a 9.4 T NMR at varying temperatures to estimate the water exchange rates.[4,5,6] The sealed samples were made up in a glove box under $N_2$ atmosphere with 2 % $H_2{}^{17}O$ with 20 % dioxane and filled the spherical bulb that fits on a 10 mm NMR tube. The NMR tube was filled with anhydrous methanol to the desired volume that fills the NMR coil inside the magnet, and was used as an internal control to measure the temperature and as an external reference for the $^{17}O$ chemical shift. The temperature dependence of the $^{17}O$ linewidths were fitted using nonlinear least-squares MATLAB fit using the following equations. The equations and parameters are explained in detail in [6].

$$\frac{1}{\tau_m} = k_{ex} = \frac{k_{ex}^{298} T}{298.15} exp\left[\frac{\Delta H_M}{R}\left(\frac{1}{298.15} - \frac{1}{T}\right)\right]$$

$$\frac{1}{\tau_v} = \frac{(t_v^{298})^{-1} T}{298.15} exp\left[\frac{\Delta H_v}{R}\left(\frac{1}{298.15} - \frac{1}{T}\right)\right]$$

$$\Delta\omega_m^0 = \frac{g_e \mu_B S(S+1) B_0 A/\hbar}{3 k_b T}$$

$$T_{1e}^{-1} = \frac{1}{25}\Delta^2 \tau_v^{-1}(4S(S+1) - 3)\left[\left(\frac{1}{1+\omega_s^2\tau_v^2}\right) + \left(\frac{4}{1+4\omega_s^2\tau_v^2}\right)\right]$$

$$T_{2e}^{-1} = \frac{1}{50}\Delta^2 \tau_v^{-1}(4S(S+1) - 3)\left[\left(3 + \frac{5}{1+\omega_s^2\tau_v^2}\right) + \left(\frac{2}{1+4\omega_s^2\tau_v^2}\right)\right]$$

$$\tau_{E1}^{-1} = T_{1e}^{-1} + \tau_m^{-1}$$

$$\tau_{E2}^{-1} = T_{2e}^{-1} + \tau_m^{-1}$$

$$R_{2m}^0 = \frac{1}{3}\left(\frac{A}{\hbar}\right)^2 S(S+1)\left[\frac{(\tau_{E1}^{-1} + \tau_{E2}^{-1})}{1+\omega_S^2\tau_v^2}\right]$$

$$R_{2p} = q\frac{c}{55.5}\tau_m^{-1}\left[\frac{(R_{2m}^0)^2 + \tau_m^{-1}R_{2m}^0 + \tau_m^{-1}}{(R_{2m}^0 + \tau_m^{-1})^2 + (\Delta\omega_m^0)^2}\right]$$

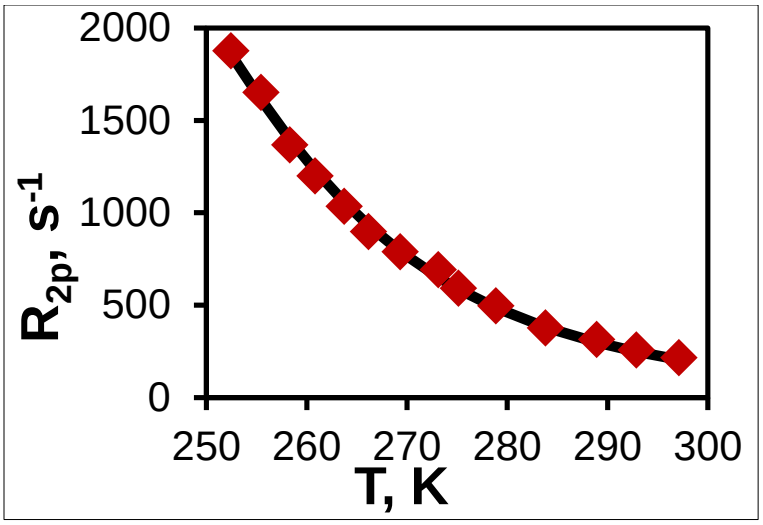


**Figure S3.** Fitting of the $^{17}O$ linewidth of the bulk water of a 40 mM $Eu^{2+}DOTA(gly)_4$ in $H_2O$, 2 % $^{17}O$ water, 20 % dioxane at different temperatures (points) and best fit (line) on a 9.4 T NMR.

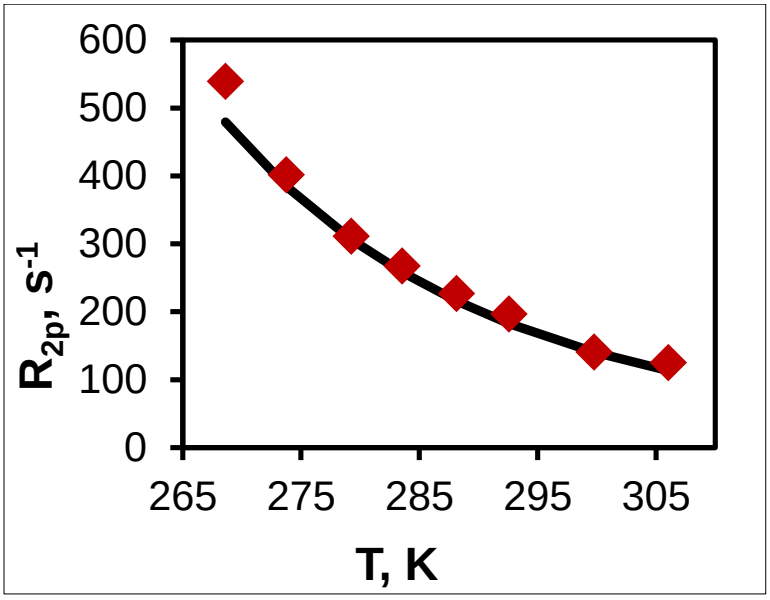


**Figure S4.** Fitting of the $^{17}O$ linewidth of the bulk water of a 90 mM $Eu^{2+}DOTA$ in $H_2O$, 2 % $^{17}O$ water, 20 % dioxane at different temperatures (points) and best fit (line) on a 9.4 T NMR.

**Table S2**. Fitting results for the water exchange rates for $Eu^{2+}$DOTA and $Eu^{2+}$DOTA$(gly)_4$ at 9.4 T in 2 % $^{17}O$ water and 20 % dioxane. The concentration, c, the water lifetime, $\tau_m$, and the enthalpy of activations, $\Delta H_{m,}$ were varied, while the remaining parameters were fixed. The estimated fitting error is below 20 % in all fitted parameters.

| Parameters | Eu(II)DOTA | Eu(II)DOTA-$(gly_4)$ |
|---|---|---|
| c (M) | 0.09 | 0.04 |
| q | 1 | 1 |
| $\tau_M^{298}$ (s) | 1.60E-09 | 4.71E-09 |
| $\Delta H_M$ (J $mol^{-1}$) | 2.40E+04 | 3.05E+04 |
| $\tau_V^{298}$ (s) | 2.27E-10 | 2.27E-10 |
| $\Delta H_v$ (J $mol^{-1}$) | 1.00E+03 | 1.00E+03 |
| $g_e$ | 2.0023 | 2.0023 |
| $\mu_B$ (J $T^{-1}$) | 9.27E-24 | 9.27E-24 |
| S | 3.50 | 3.50 |
| $B_0$ (T) | 9.40 | 9.40 |
| $\kappa_b$ (J $K^{-1}$) | 1.38E-23 | 1.38E-23 |
| A / ħ (rad $s^{-1}$) | -3.30E+06 | -3.30E+06 |
| $\varpi_H$ (Hz) | 2.51E+09 | 2.51E+09 |
| $\varpi_S$ (Hz) | 1.66E+12 | 1.66E+12 |
| $\Delta^2$ ($s^{-2}$) | 1.9E+20 | 1.9E+20 |

**Table S3.** Individual calculated parameters of the fitting procedure and chemical shift values for $Eu^{2+}$DOTA.

| $\delta_O$ | T,K | Lw | $R_{2r}$ (exp) | $R_{2p}^O$(cal) | $(\tau_M)^{-1}$ | $(\tau_V)^{-1}$ | $\Delta\omega_M^O$ | $(T_{1E})^{-1}$ | $(T_{2E})^{-1}$ | $(\tau_{E1})^{-1}$ | $(\tau_{E2})^{-1}$ | $R_{2M}^O$ |
|---|---|---|---|---|---|---|---|---|---|---|---|---|
| ppm | K | Hz | $s^{-1}$ | $s^{-1}$ | $s^{-1}$ | $s^{-1}$ | rad $s^{-1}$ | $s^{-1}$ | $s^{-1}$ | $s^{-1}$ | $s^{-1}$ | $s^{-1}$ |
| 4.3 | 268.6 | 265.9 | 539.1 | 479.4 | 1.94E+08 | 2.55E+09 | -8.15E+05 | 8.48E+05 | 2.69E+11 | 1.95E+08 | 2.69E+11 | 2.93E+05 |
| 4.4 | 273.8 | 213.9 | 401.8 | 384.8 | 2.42E+08 | 2.82E+09 | -8.00E+05 | 9.40E+05 | 2.42E+11 | 2.43E+08 | 2.43E+11 | 2.35E+05 |
| 4.0 | 279.3 | 176.9 | 311.1 | 306.6 | 3.04E+08 | 3.14E+09 | -7.84E+05 | 1.05E+06 | 2.18E+11 | 3.05E+08 | 2.18E+11 | 1.87E+05 |
| 4.1 | 283.6 | 157.2 | 267.2 | 258.1 | 3.61E+08 | 3.40E+09 | -7.72E+05 | 1.13E+06 | 2.01E+11 | 3.62E+08 | 2.01E+11 | 1.58E+05 |
| 3.8 | 288.2 | 138.5 | 226.6 | 215.9 | 4.32E+08 | 3.70E+09 | -7.60E+05 | 1.23E+06 | 1.85E+11 | 4.33E+08 | 1.85E+11 | 1.32E+05 |
| 3.7 | 292.6 | 123.9 | 196.7 | 182.7 | 5.10E+08 | 4.00E+09 | -7.49E+05 | 1.33E+06 | 1.71E+11 | 5.11E+08 | 1.71E+11 | 1.12E+05 |
| 3.6 | 299.8 | 98.5 | 140.4 | 140.8 | 6.62E+08 | 4.53E+09 | -7.31E+05 | 1.51E+06 | 1.51E+11 | 6.63E+08 | 1.52E+11 | 8.62E+04 |
| 3.3 | 306.1 | 87.9 | 125.0 | 113.1 | 8.24E+08 | 5.02E+09 | -7.16E+05 | 1.67E+06 | 1.36E+11 | 8.26E+08 | 1.37E+11 | 6.92E+04 |

**Table S4**. Individual calculated parameters of the fitting procedure and chemical shift values of $Eu^{2+}DOTA(gly)_4$.

| $\delta_O$ | T,K | Lw | $R_{2r}$ (exp) | $R_{2p}^O$(cal) | $(\tau_M)^{-1}$ | $(\tau_V)^{-1}$ | $\Delta\omega_M^O$ | $(T_{1E})^{-1}$ | $(T_{2E})^{-1}$ | $(\tau_{E1})^{-1}$ | $(\tau_{E2})^{-1}$ | $R_{2M}^O$ |
|---|---|---|---|---|---|---|---|---|---|---|---|---|
| ppm | K | Hz | $s^{-1}$ | $s^{-1}$ | $s^{-1}$ | $s^{-1}$ | rad $s^{-1}$ | $s^{-1}$ | $s^{-1}$ | $s^{-1}$ | $s^{-1}$ | $s^{-1}$ |
| 5.1 | 252.5 | 754.3 | 1876.0 | 1854.9 | 1.94E+07 | 1.80E+09 | -8.68E+05 | 6.29E+04 | 4.01E+10 | 1.94E+07 | 4.01E+10 | 2.94E+06 |
| 4.6 | 255.5 | 674.2 | 1650.4 | 1611.9 | 2.33E+07 | 1.92E+09 | -8.57E+05 | 6.74E+04 | 3.75E+10 | 2.33E+07 | 3.75E+10 | 2.45E+06 |
| 4.9 | 258.4 | 576.4 | 1367.1 | 1396.2 | 2.76E+07 | 2.05E+09 | -8.48E+05 | 7.18E+04 | 3.51E+10 | 2.77E+07 | 3.52E+10 | 2.06E+06 |
| 5.1 | 260.9 | 516.6 | 1198.7 | 1229.0 | 3.20E+07 | 2.16E+09 | -8.40E+05 | 7.58E+04 | 3.33E+10 | 3.21E+07 | 3.33E+10 | 1.78E+06 |
| 4.8 | 263.8 | 457.4 | 1034.2 | 1057.4 | 3.77E+07 | 2.30E+09 | -8.30E+05 | 8.07E+04 | 3.13E+10 | 3.78E+07 | 3.13E+10 | 1.51E+06 |
| 4.6 | 266.2 | 408.7 | 898.6 | 931.1 | 4.33E+07 | 2.42E+09 | -8.23E+05 | 8.49E+04 | 2.97E+10 | 4.33E+07 | 2.98E+10 | 1.32E+06 |
| 4.6 | 269.3 | 366.8 | 787.9 | 790.6 | 5.14E+07 | 2.58E+09 | -8.13E+05 | 9.05E+04 | 2.79E+10 | 5.15E+07 | 2.79E+10 | 1.11E+06 |
| 4.4 | 273.1 | 328.6 | 692.3 | 649.7 | 6.30E+07 | 2.79E+09 | -8.02E+05 | 9.77E+04 | 2.58E+10 | 6.31E+07 | 2.59E+10 | 9.06E+05 |
| 4.5 | 275.2 | 292.3 | 590.4 | 585.3 | 7.01E+07 | 2.90E+09 | -7.96E+05 | 1.02E+05 | 2.48E+10 | 7.02E+07 | 2.49E+10 | 8.14E+05 |
| 4.6 | 278.9 | 255.6 | 496.3 | 485.2 | 8.49E+07 | 3.12E+09 | -7.85E+05 | 1.09E+05 | 2.31E+10 | 8.50E+07 | 2.32E+10 | 6.73E+05 |
| 4.3 | 283.9 | 209.0 | 376.2 | 380.0 | 1.09E+08 | 3.42E+09 | -7.72E+05 | 1.20E+05 | 2.10E+10 | 1.09E+08 | 2.11E+10 | 5.25E+05 |
| 4.2 | 289.0 | 181.5 | 314.3 | 297.7 | 1.39E+08 | 3.75E+09 | -7.58E+05 | 1.32E+05 | 1.92E+10 | 1.39E+08 | 1.93E+10 | 4.11E+05 |
| 4.0 | 292.9 | 157.3 | 256.1 | 247.5 | 1.67E+08 | 4.03E+09 | -7.48E+05 | 1.41E+05 | 1.79E+10 | 1.67E+08 | 1.80E+10 | 3.41E+05 |
| 3.9 | 297.2 | 138.6 | 214.8 | 204.2 | 2.03E+08 | 4.33E+09 | -7.37E+05 | 1.52E+05 | 1.66E+10 | 2.03E+08 | 1.68E+10 | 2.82E+05 |

**Cyclic voltammetry**

The cyclic voltammetry experiments with $Eu^{3+}DOTA(gly)_4$ were performed on 10 mM solutions in degassed water in the presence of 100 mM of KCl as a supporting electrolyte. Standard glassy carbon electrode, $Ag^{+}/AgCl$ electrode and platinum wire was used as working electrode, reference electrode, and counter electrode, respectively. The voltammograms were recorded at different scan rates from 100 to 500 mV/min scan rate. All cyclic voltammetry experiments were conducted in an inert $N_2$ atmosphere.

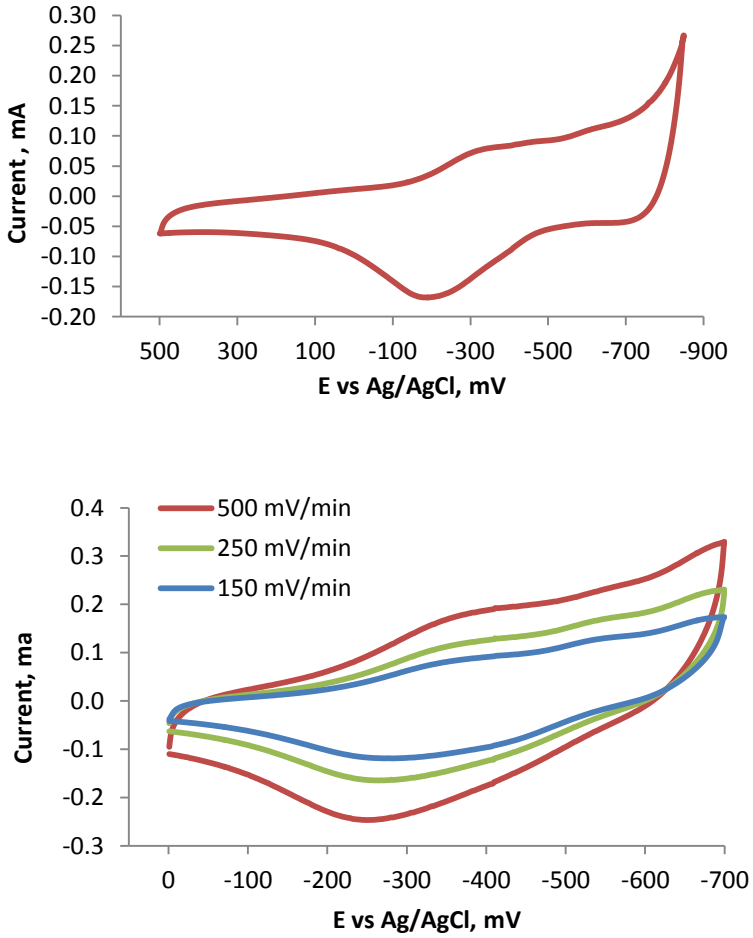


**Figure S5.** Cyclic voltammogram of $Eu^{3+}DOTA(gly)_4$ at 100 mV/min (top) and at different scan rates (150, 250 and 500 mV/min). The conditions for reversibility are not attained even at higher scan rates.

**Closed system stability**

The NMR samples of $Eu^{2+}DOTA(gly)_4$ and $Eu^{2+}DOTA$ in 3 mm NMR tubes were prepared in degassed water at pH =7 in a glove box under $N_2$ atmosphere. The $T_1$ relaxation times were measured at 20°C over a period of 104 days for $Eu^{2+}DOTA(gly)_4$ and 44 days for $Eu^{2+}DOTA$. 1

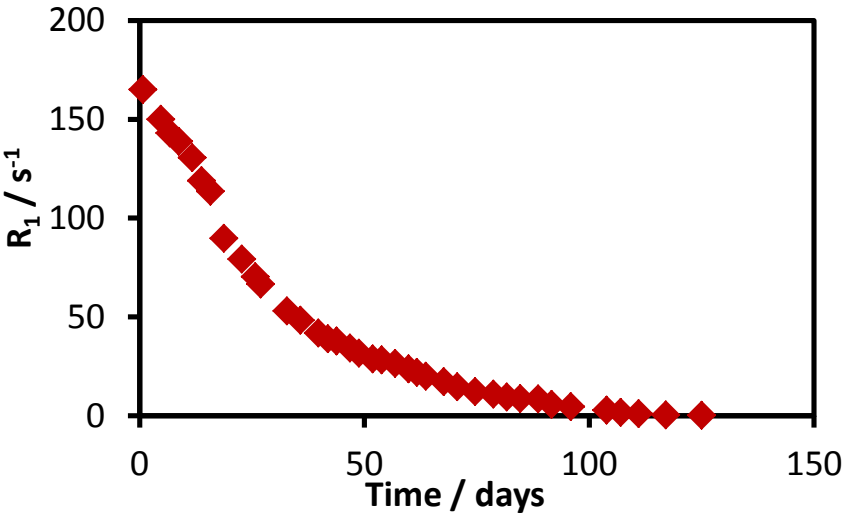


**Figure S6.** Decay of the bulk water relaxation rates in a $Eu^{2+}DOTA(gly)_4$ solution (60 mM) in a closed system under an inert atmosphere at 9.4 T.

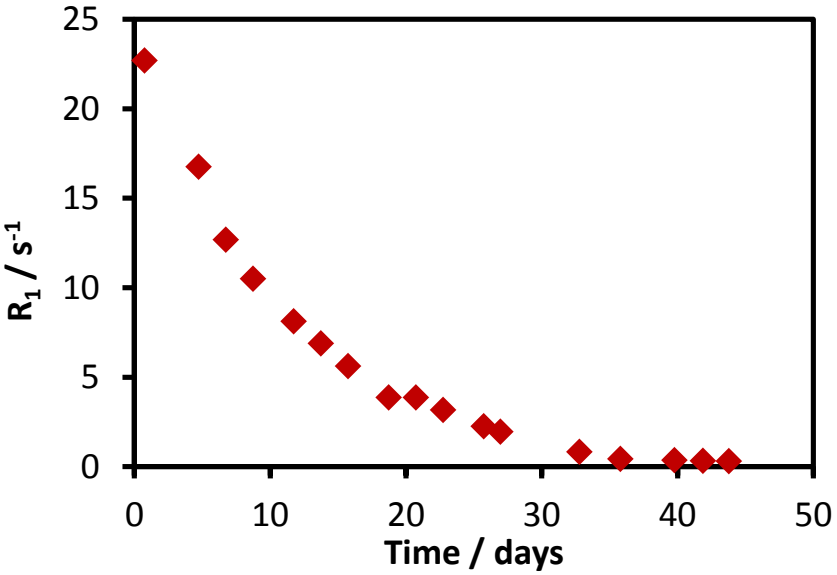


**Figure S7.** Decay of the bulk water relaxation rates in a $Eu^{2+}DOTA$ solution (60 mM) in a closed system under an inert atmosphere at 9.4 T**.**

**Open system stability**

Three phantoms were prepared (1 cm diameter, 2 cm length) and filled with $H_2O$, $Eu^{3+}DOTA(gly)_4$ (10mM) and $Eu^{2+}DOTA(gly)_4$ (15mM). The $Eu^{2+}$ solution was prepared in a glove box and sealed before removing it from the inert atmosphere. The phantoms were placed vertically in the imaging system. After an initial scan, the cap of the sealed $Eu^{2+}DOTA(gly)_4$ solution was removed and immediately put back in the scanner. $T_1$w images and paraCEST images were obtained every 10 minutes for 140 minutes. The $T_1$w images were obtained using a FSEMS sequence with TR = 5 ms, ESP = 15 ms, ETL = 2, kzero = 1, effective TE = 40 ms, a data matrix of 256 x 256, a FOV of 35 x 35 $mm^2$, 4 averages and a total acquisition time of 42 s. The $T_1$ map was obtained using a FLAIR sequence, with TR = 4 s, ESP = 10 ms, ETL = 8, kzero = 4 and effective TE = 40 ms. The CEST images were obtained using the same sequence and slice settings, but a TR = 2 s, ESP = 6.7 ms, ETL = 8, k zero = 4, effective TE = 26.6 ms and a saturation power of 10 μT, saturation frequencies of 54 (on-resonance) and -54 ppm (off-resonance), a saturation time of 3 s, a data matrix of 128 x 128, 2 averages and a total acquisition time of 2 minutes and 20 seconds. The $T_1$ map was obtained using the same slice setting, but was obtained by using an inversion recovery sequence with a minimum of 8 different data points.

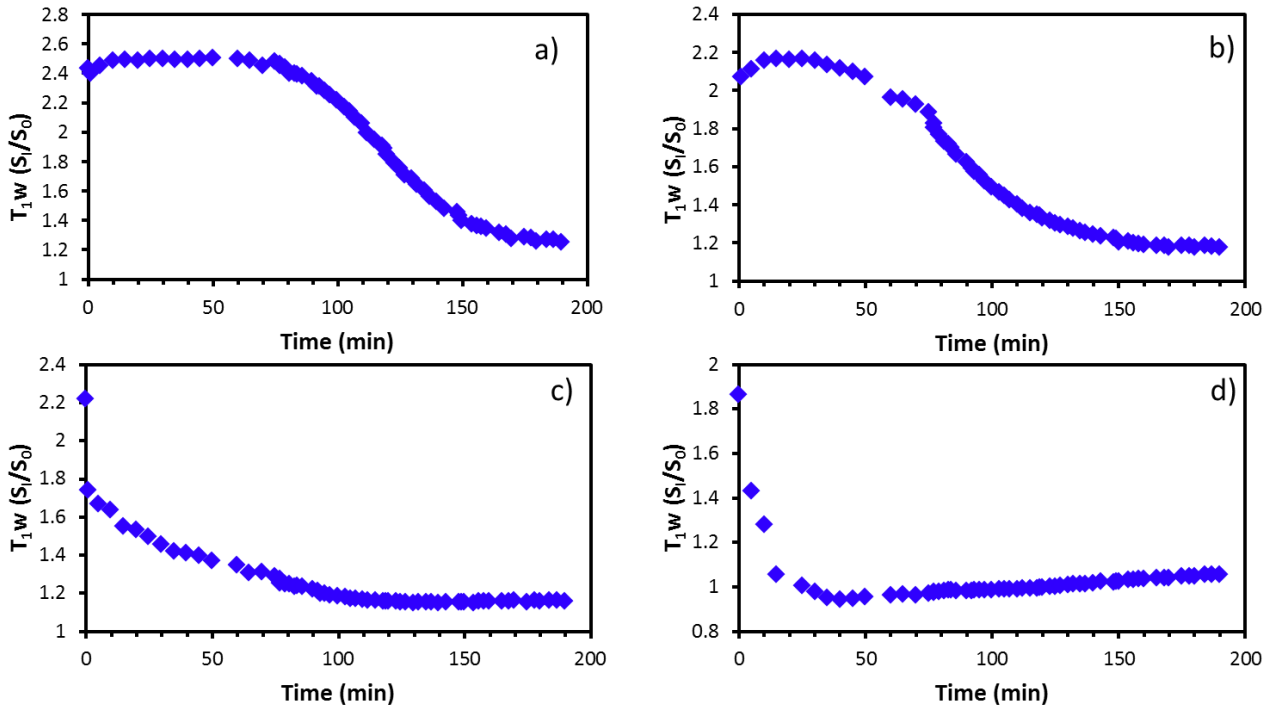


**Figure S8.** Decay of the $T_1$w intensity of open system phantoms containing $Eu^{2+}DOTA(gly)_4$ at a) 4 mm, b) 3 mm, c) 2 mm and d) 1 mm away from the surface.

**Oxidation with $H_2O_2$**

A phantom (1 cm diameter, 1.5 cm length) was filled with $Eu^{2+}DOTA(gly)_4$ (10 mM, 1 mL) in the glove box. A tube for injecting the $H_2O_2$ (3 % solution in water) and an exhaust tube were inserted through the lid. The sealed container was placed vertically in the imaging system. The $H_2O_2$ was injected at 120 µL / min for 20 seconds to ensure oxidation of the $Eu^{2+}$ agent. Consequtive sagittal $T_1$w images and PARACEST images were recorded every 2.5 minutes for 60 minutes. The $T_1$w images were obtained using a FSEMS sequence with TR = 500 ms, ESP = 15 ms, ETL = 2, kzero = 1, effective TE = 15 ms, a data matrix of 256 x 256, a FOV of 50 x 50 $mm^2$, 4 averages and a total acquisition time of 42 seconds. The CEST images were obtained using the same sequence and slice settings, TR=2 s, ESP=6.4 ms, ETL=8, kzero=4, effective TE = 25.4 ms, a saturation power of 10 µT, saturation time = 3 s, saturation frequencies of 54 ppm (on-resonance) and -54 ppm (off resonance), a data matrix of 128 x 128, 2 averages and a total acquisition time of 2 minutes 20 seconds.

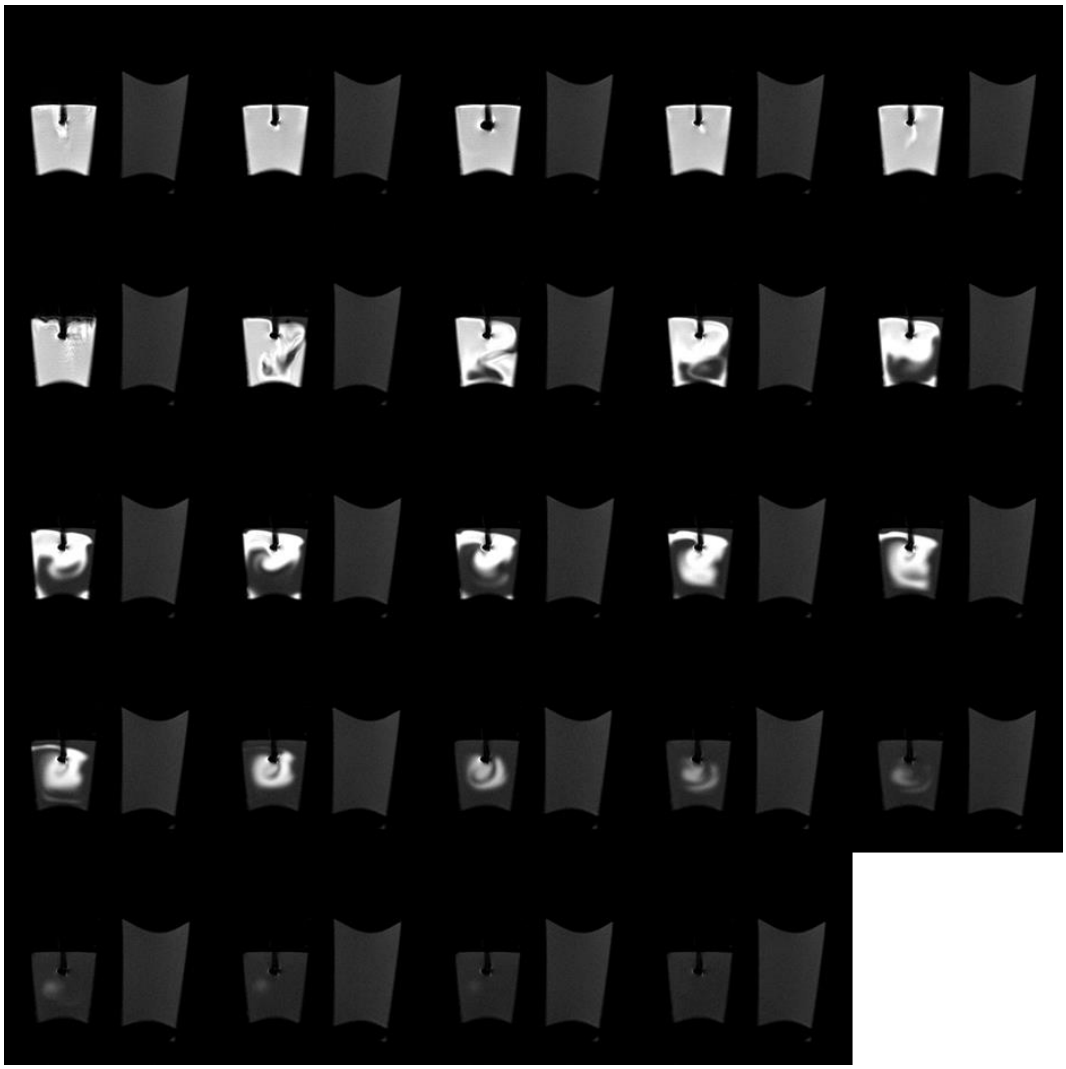

**Figure S9.** $T_1$w images acquired of the forced oxidation of $Eu^{2+}$DOTA(gly)$_4$ (left) with $H_2O$ as a reference (right) at 2.5 minute intervals.

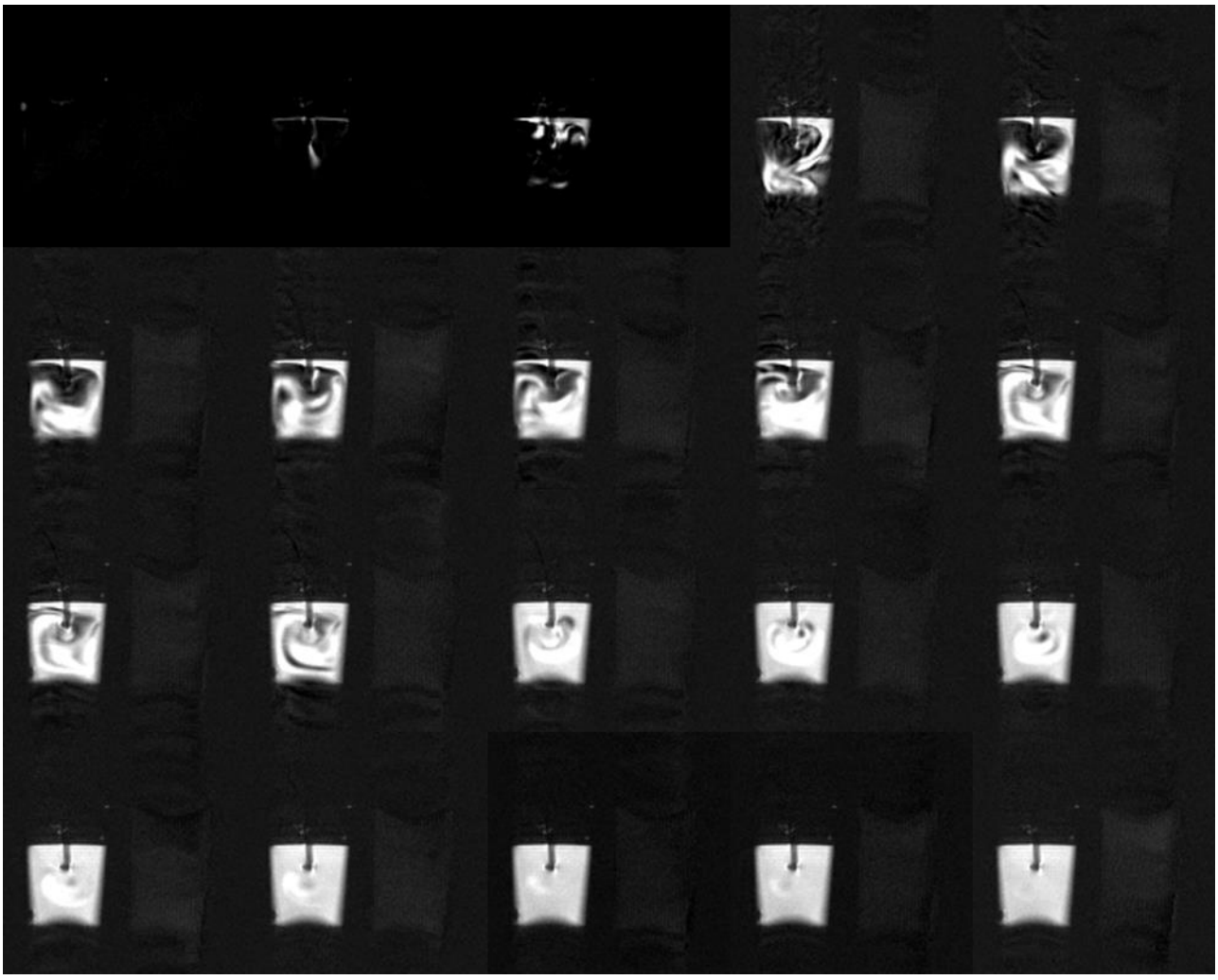

**Figure S10.** paraCEST images (off-resonance and on-resonance images subtracted) acquired of the forced oxidation of $Eu^{2+}DOTA(gly)_4$ (left) with $H_2O$ as a reference (right) at 2.5 minute intervals.

**Animal experiments**

**Animal models**

All animal experiments were conducted to according to the standards of the University of Texas Southwestern Medical Center Institutional Animal Care and Use Committee. Female C57/blk6 mice of 6 – 10 weeks of age were used for the imaging.

**Imaging experiments**

Animals were anesthetized with isoflurane (1-2 % in medical oxygen) and probes were placed on the skin to monitor temperature and on the chest to monitor respiration. Each animal experiment was performed at least four times.

$Eu^{2+}DOTA(gly)_4$ (10 mM, 100 µL, 0.05 mmol / kg dose) was administered intramuscularly into the thigh. $T_1w$ imaging experiments were performed on the 9.4 T imaging system using a ge3D sequence with a TR = 3.6 ms, TE = 1.8 ms, a FOV of 35 x 75 x 75 $mm^3$, a flip angle of 20°, a data matrix of 128 x 128 x 128, 4 averages and a total acquisition time of 3 minutes 40 seconds. The CEST images were obtained using a FSEMS sequence with TR = 2 s, ESP = 6.5 ms, ETL = 8, kzero = 4, effective TE = 25.8 ms , a FOV of 30 x 30 $mm^2$, a data matrix of 128 x 128, 4 averages, saturation power = 10 µT, saturation frequency 42 (on-resonance) and -42 ppm (off-resonance), saturation time = 3s and a total acquisition time of 31 seconds. Note that the chemical shift of the bound water CEST peak is temperature dependent. For $Eu^{3+}DOTA(gly)_4$ it is 42 ppm at 37 ºC and 54 at 20 °C.

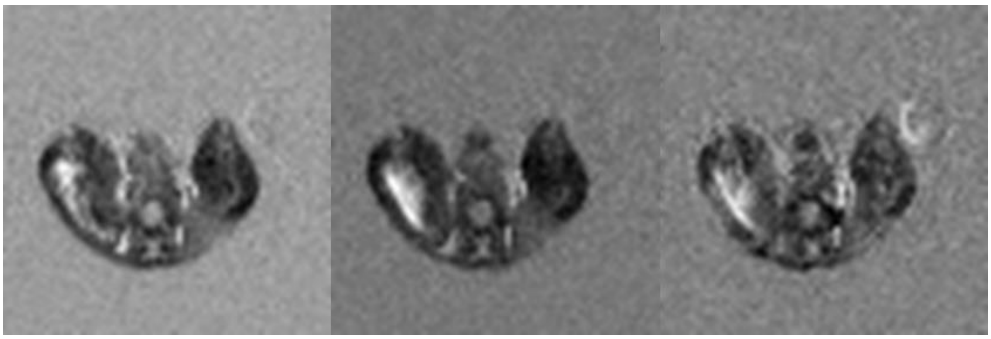

**Figure S11.** PARACEST imaging of the thigh muscle after injected $Eu^{2+}DOTA(gly)_4$ at 12, 17 and 23 minutes.

**References**


[1] Zhang S, Wu K, Biewer MC, Sherry AD, *Inorg. Chem.* **2001**; *40*, 4284–4290.

[2] Desreux J.F., *Inorg Chem*. **1980**, *19*, 1319-1324

[3] Zucchi G, Thuéry P, Rivière E, Ephritikhine M, *Chem. Commun*. **2010**, *46*, 9143–9145.

[4] Seibig S, Toth E, Merbach AE, *J. Am. Chem. Soc.* **2000***, 122, 5822-5830*

[5] Micskei K, Helm L, Brucher E, Merbach A.E.*, Inorg Chem.*, **1993**, *32*, 3844-3850

[6] Helm. L, Merbach A.E., *Coord. Chem. Rev.*, **1999**, *187*, 151-181.

## Appendix

### 1. Color version of figures in manuscript:

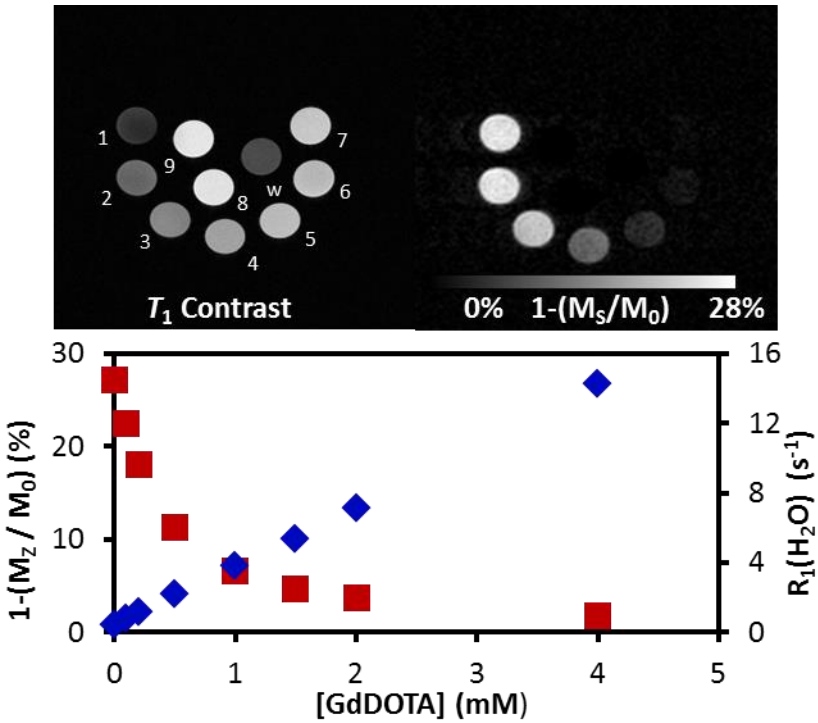


**Figure 2. (Top)** Correlation between relaxation rates (diamonds) and the CEST effect (squares) in a mixture of $Gd^{3+}$**1** and $Eu^{3+}$**2**. Each circle in the image represents a separate sample. [$Eu^{3+}$**2**] in each sample was 10 mM while [$Gd^{3+}$**1**] ranged from 0 to 4 mM. Vial 9 contained 8 mM $Gd^{3+}$**1** alone while vial w contained only water. **(Bottom)** Plots of CEST (1-($M_S$/$M_0$)) and $R_1$ versus [$Gd^{3+}$**1**]. Imaging parameters: $B_0$=9.4 T, 20 °C; $T_1$w: GEMS sequence, TR= 9.9 ms, TE= 5.0 ms; CEST: FSEMS sequence, sat time = 3 s, sat power = 10 μT, sat frq = 54 (on),-54 ppm (off-resonance).

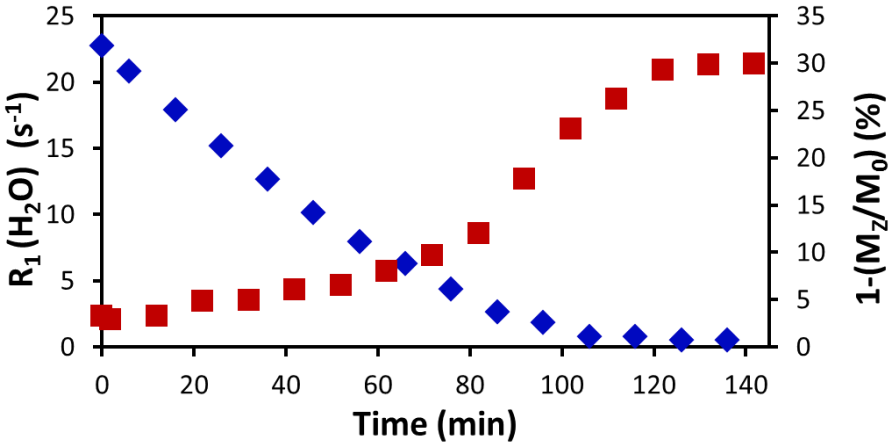


**Figure 3.** Plots of relaxation rate ($R_1$) (diamonds) and CEST (squares) for a solution initially containing 10 mM $Eu^{2+}$**2** versus time. The data were collected from images in a single slice 4 mm away from the surface. Imaging parameters: $B_0$=9.4 T, 20 °C, $T_1$w: FSEMS sequence, TR = 2 s, TE = 3.0 ms; CEST: FSEMS sequence, sat time = 3 s, sat power = 10 μT, sat frq = 54 (on-resonance), -54 ppm (off-resonance).